IEEE Access
Multidisciplinary ⁝ Rapid Review ⁝ Open Access Journal

Digital Object Identifier

Fixed-Time Sliding Mode Control for Vehicle Platoon with Input Dead-Zone and Prescribed Performance

Yongqiang Jiang[1,2,3], Yiguang Wang[1,2,3], Xiaojie Li[1,2,3*], Xiaoyan Zhan[1,2,3], and Xubing Tang[1,2,3]
[1]Key Laboratory of Advanced Manufacturing and Automation Technology, Guilin University of Technology, Guilin 541006, China
[2]Guangxi Engineering Research Center of Intelligent Rubber Equipment, Guilin University of Technology, Guilin 541006, China
[3]College of Mechanical and Control Engineering, Guilin University of Technology, Guilin 541006, China

Corresponding author: Xiaojie Li (e-mail: xiaojie_li@foxmail.com).

This work was supported in part by the Fund of Guangxi Science and Technology Key Research and Development Program under Grant 2024AB3321, in part by the Fund of Guilin Science Research and Technology Development Program under Grant 20230110-4 and 20230105-3, and in part by the Fund of Innovation Project of Guangxi Graduate Education under Grant JGY2023151.

ABSTRACT This article studies the fixed-time sliding mode control (FTSMC) issue for vehicle platoon with prescribed performance, input dead-zone (IDZ), unknown nonlinearities, and external disturbances. Unlike the traditional funnel-shaped prescribed performance function, a new tunnel fixed-time prescribed performance function (TFTPPF) is proposed, which defines more compact tunnel-shaped performance boundaries that can accelerate convergence speed and reduce overshoot of tracking error. The convergence time of TFTPPF is predefined and is independent of control parameters, which enhances the design flexibility of performance function. Furthermore, Chebyshev neural network (CNN) is adopted to approximate unknown nonlinearities, and new adaptive mechanisms are designed to estimate IDZ slope and external disturbances. Utilizing the proposed TFTPPF, CNN, and adaptive mechanisms, a novel FTSMC strategy for vehicle platoon is proposed to ensure string stability and achieve predefined tracking performance within a fixed time. Finally, comparative numerical examples are employed to validate the validity and advantages of the proposed strategy.

INDEX TERMS Vehicle platoon control, input dead-zone, fixed-time sliding mode, unknown nonlinearities, prescribed performance control.

I. INTRODUCTION

Recently, the rapid increase in the number of automobiles has caused numerous traffic issues, including traffic congestion, energy consumption, and exhaust emissions [1]–[4]. Vehicle platoon control is receiving widespread attention for its benefits in enhancing traffic efficiency, improving driving safety, optimizing resource utilization efficiency, and reducing carbon emissions [5]–[7]. Many control issues of vehicle platoon have been studied, including heterogeneity in dynamics [8], information flow topology [9], spacing policy [10], etc.

Vehicles are inevitably impacted by external disturbances and unknown nonlinearities, potentially compromising the control performance of vehicle platoon [11]–[14]. To mitigate the impact of external disturbances and unknown nonlinearities on system performance, several methods have been developed, for example iterative proportional-integral observer [15], [16], H_∞ control [17], model predictive control [18], and disturbance observer [19], [20], etc. In these studies, due to the fact that sliding mode control (SMC) possesses strong robustness and insensitivity to nonlinearities and disturbances, it is widely applied in vehicle platoon control [21], [22]. In [21], a distributed adaptive SMC strategy is designed for vehicle platoon with unknown nonlinearities to guarantee that follower vehicles track the leader well. In [22], an integral SMC is designed to ensure that vehicle maintains predefined spacing from the adjacent vehicles. However, one issue with the aforementioned traditional SMC is that they are unable to predesign convergence time of tracking error for vehicle platoon, which may lead to delayed system response, increased accident risks, and reduced road safety in complex traffic environments [23], [24]. Therefore, it is necessary to develop a new SMC strategy for vehicle platoon to ensure convergence of tracking error within a fixed time.

The input dead-zone (IDZ) frequently occurs in the actuators of vehicle platoon, which reduces the system precision and may even result in system instability [25]–[27]. To mitigate the negative impacts of IDZ on the vehicle platoon, researchers have conducted extensive research on it [28], [29].

This article has been accepted for publication in IEEE Access. This is the author's version which has not been fully edited and content may change prior to final publication. Citation information: DOI 10.1109/ACCESS.2025.3535827

In [28], by assuming that IDZ slope is a positive constant, an adaptive strategy is designed to achieve velocity synchronization with the leader. In [29], a feedback linearization strategy is proposed to achieve control objectives based on the assumption that IDZ slope is strictly monotonic. It is worth noting that the practical applications of the above methods are constrained by the assumption of IDZ slope. Additionally, the lack of performance constraints in the vehicle platoon may lead to deviations between the actual system performance and expectations, or even result in failure to meet the expected performance indicators.

To ensure that the vehicle platoon possesses predetermined performance, prescribed performance control (PPC) is developed, which utilizes the predetermined performance indicators as controller parameters to guarantee that the system achieves the desired performance [30], [31]. In [30], a distributed PPC strategy for vehicle platoon is developed to guarantee that tracking error does not exceed a predetermined boundary, the convergence speed is no less than a given lower bound, and the steady-state error converges within a predefined range. In [31], PPC method is applied in vehicle platoon with input delay to ensure that the system possesses predefined performances. The convergence time of prescribed performance function (PPF) in traditional PPC approaches infinity. However, in most applications, it is desirable for system state to reach a predefined range within a predetermined time [32]. In [33], a fixed-time PPC strategy is designed to guarantee that tracking error of vehicle platoon converges to a predefined range within a fixed time. It is worth noting that the performance boundaries of the aforementioned PPC are distributed on different sides of the coordinate system and present a loose funnel shape, which cannot effectively ensure that the overshoot of tracking error is small or zero. Therefore, it is essential to develop a new PPC strategy to reduce overshoot, while enhancing system performance.

In light of the aforementioned discussion, a novel control strategy for vehicle platoon with prescribed performance, IDZ, unknown nonlinearities, and external disturbances is developed to guarantee string stability and achieve predefined tracking performance within a fixed time. Chebyshev neural network (CNN) is utilized to approximate unknown nonlinearities and new adaptive mechanisms are designed to estimate IDZ slope and external disturbances, thereby effectively reducing the negative impacts of unknown nonlinearities, IDZ, and external disturbances on the system performance. The advantages of this scheme are outlined below.

1) A new tunnel fixed-time prescribed performance function (TFTPPF) is proposed, which defines performance boundaries that are located on the same side of the coordinate system and are more compact, thereby reducing the overshoot of vehicle platoon and enhancing the tracking performance.
2) CNN is employed to approximate unknown nonlinearities in vehicle platoon, and adaptive mechanisms are designed to estimate IDZ slope and external disturbances, which effectively mitigate the adverse impacts of unknown nonlinearities, IDZ, and external disturbances on system performance.
3) Based on the proposed TFTPPF, CNN, and adaptive mechanisms, a novel fixed-time sliding mode control (FTSMC) strategy is designed to ensure string stability of vehicle platoon and achieve predetermined tracking performance within a fixed time.

The remainder of this paper is organized as follows. Section II introduces the dynamic model of vehicle and PPC. Section III gives the design process of the controller and the stability analysis. In Section IV, the numerical examples illustrate the validity and superiority of the designed strategy. Section V summarizes the conclusions.

II. PROBLEM STATEMENT

A. VEHICLE DYNAMICS

As depicted in Figure. 1, a vehicle platoon is comprised of one leader (vehicle 0) and N follower vehicles, and each vehicle can obtain information from adjacent vehicles.The dynamic model of the following vehicle i $(i = 1, 2, \dots, N)$ is as follow

$$\begin{aligned}\dot{x}_i(t) =& v_i(t)\\ \dot{v}_i(t) =& a_i(t)\\ \dot{a}_i(t) =& Dz(u_i(t)) + D_i(t) - \frac{1}{m_i\tau_i}\Big[\rho_a A_i C_{di}(\frac{1}{2}v_i^2(t)\\ &+ \tau_i v_i(t)a_i(t)) + \wp_i\Big] - \frac{1}{\tau_i}a_i(t)\\ =& Dz(u_i(t)) + D_i(t) + f_i(v_i(t), a_i(t))\end{aligned} \tag{1}$$

where $x_i(t)$, $v_i(t)$, and $a_i(t)$ denote the ith vehicle's position, velocity, and acceleration, respectively; m_i represents mass; τ_i is the engine time constant; ρ_a denotes air density; A_i represents the cross-sectional area; the road slope term $\wp_i = m_i g\sin\phi + m_i g \ell_i \cos\phi$, with g being the acceleration of the gravity, ϕ represents the angle of the road slope, and ℓ_i denotes the rolling resistance coefficient; C_{di} denotes the air drag coefficient; the external disturbances $D_i(t)$ are bounded as $|D_i(t)| \le \bar{D}_i$, with $\bar{D}_i > 0$. In practice, since $\rho_a, A_i, C_{di}, \tau_i, \ell_i$, and ϕ are often difficult or even impossible to obtain directly, the nonlinearities $f_i(v_i(t), a_i(t))$ are assumed to be unknown. $Dz(u_i(t))$ is the control input as

$$Dz(u_i(t)) = \begin{cases} z_{i,r}(u_i(t) - \gamma_{i,r}), & u_i(t) \ge \gamma_{i,r}\\ 0, & -\gamma_{i,l} < u_i(t) < \gamma_{i,r}\\ z_{i,l}(u_i(t) + \gamma_{i,l}), & u_i(t) \le \gamma_{i,l}\end{cases} \tag{2}$$

where $\gamma_{i,r}$ and $\gamma_{i,l}$ denote the breakpoints of IDZ, $z_{i,r}$ and z_{i,l_1} are the IDZ slopes. To streamline the notation, we adopt $\bullet$ as a representation for $\bullet(\cdot)$.

The leader can be described as

$$\begin{aligned}\dot{x}_0 &= v_0\\ \dot{v}_0 &= a_0\end{aligned} \tag{3}$$

To ensure traffic safety, a quadratic spacing policy (QSP) is designed as

$$e_i = d_i - w_i - h_1 v_i - h_2 v_i^2 - \mu \tag{4}$$

This article has been accepted for publication in IEEE Access. This is the author's version which has not been fully edited and content may change prior to final publication. Citation information: DOI 10.1109/ACCESS.2025.3535827

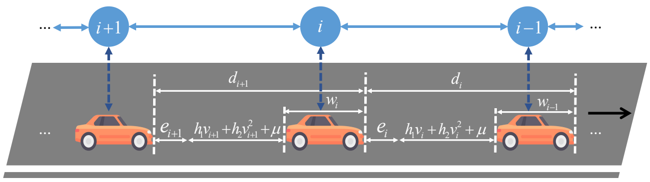

FIGURE 1: The communication topology of vehicle platoon.

where $d_i = x_{i-1} - x_i$, e_i is the tracking error, w_i represents the length of vehicle, $h_1 > 0$, $h_2 > 0$, and μ denotes the standstill spacing.

B. PRESCRIBED PERFORMANCE

For traditional PPC, the performance boundaries are given by [34]

$$\begin{cases} -\Omega\Xi_i \le e_i \le \Xi_i,\ e_i(0) \ge 0 \\ -\Xi_i \le e_i \le \Omega\Xi_i,\ e_i(0) < 0 \end{cases} \tag{5}$$

where $\Xi_i = (\Xi_{i,0} - \Xi_{i,\infty})e^{-\partial_i t} + \Xi_{i,\infty}$ denotes PPF; $\partial_i > 0$, Ω is a design parameter with $0 < \Omega \le 1$, $\Xi_{i,\infty} = \lim_{t\to\infty} \Xi_i(t) > 0$, and $\Xi_{i,0} = \Xi_i(0) > e_i(0) \ge 0$.

According to (5), the tracking trajectories of e_i and PPF are presented in Figure. 2. From Figure. 2, although traditional PPC can ensure that e_i converges within the range defined by the performance boundaries, there are still some problems. 1) The performance boundaries are situated on different sides of the coordinate system, presenting a loose funnel shape, which is not conducive to achieving small overshoot or zero overshoot of e_i. 2) From (5), different initial conditions may lead to controller redesign, which is detrimental to the controller design. 3) The convergence time of traditional PPF tends to infinity. However, in most practical applications, it is desired that the system state can reach a predefined range within a predetermined time.

To address the aforementioned issues, the new performance boundaries are proposed as

$$\rho_{i,l} < e_i < \rho_{i,r} \tag{6}$$

where $\rho_{i,l} = [\kappa_1 \operatorname{sign}(e_i(0)) - \varsigma_1]\delta_i - \delta_{i,tf} \operatorname{sign}(e_i(0))$ and $\rho_{i,r} = [\kappa_2 \operatorname{sign}(e_i(0)) + \varsigma_2]\delta_i - \delta_{i,tf} \operatorname{sign}(e_i(0))$ are the TFTPPF, with $0 < \kappa_1 < 1$, $0 < \kappa_2 < 1$, $0 < \varsigma_1 < 1$, $0 < \varsigma_2 < 1$; δ_i is defined as

$$\delta_i = \begin{cases} (\delta_{i,0} - \delta_{i,t_f})e_i^{-\varphi_i t} + \delta_{i,t_f} & 0 < t < t_f \\ \delta_{i,t_f} & t \ge t_f \end{cases}$$

where $\delta_{i,0} = \lim_{t\to 0} \delta_i > 0$, $\varphi_i > 0$, and $\delta_{i,tf} = \lim_{t\to t_f} \delta_i > 0$; $t_f > 0$ is the convergence time. Based on (6), the tracking trajectories of e_i and TFTPPF are shown in Figure. 3. Unlike (5), (6) is more concise in form without considering the sign of e_i, which simplifies the controller design. From Figure. 3, the proposed tunnel performance boundaries are more compact, which reduces overshoot of tracking error and enhances system performance. Furthermore, t_f can be predefined, independent of initial conditions or control parameters, which improves the design flexibility of PPF.

As given in (6), e_i is constrained, making it unable to be directly applied in the controller design. Therefore, e_i is transformed into an equivalent and unconstrained ω_i as

$$\omega_i = \ln\left(\frac{\theta_i}{1-\theta_i}\right) \tag{7}$$

where $\theta_i = [e_i - \rho_{i,l}]/[\rho_{i,r} - \rho_{i,l}]$.

Theorem 1: If ω_i is bounded, then e_i can converge to the predefined range defined by TFTPPF.

Proof: (7) can be rewritten as

$$e^{\omega_i} = \frac{\theta_i}{1-\theta_i} \tag{8}$$

Then, we have

$$\theta_i = \frac{e^{\omega_i}}{1+e^{\omega_i}} \tag{9}$$

As ω_i is bounded, there exists $\bar{\omega}_i > 0$ such that $-\bar{\omega}_i \le \omega_i \le \bar{\omega}_i$ holds. Then, one can obtain

$$0 < \frac{e^{-\bar{\omega}_i}}{1+e^{-\bar{\omega}_i}} \le \theta_i \le \frac{e^{\bar{\omega}_i}}{1+e^{\bar{\omega}_i}} < 1 \tag{10}$$

Based on (7) and (10), one has

$$0 < \frac{e_i - \rho_{i,l}}{\rho_{i,r} - \rho_{i,l}} < 1 \tag{11}$$

Then the inequality (6) holds. The proof is completed.

C. CONTROL OBJECTIVES

The purpose of this paper is to design a strategy for vehicle platoon to achieve the following objectives.

- Individual stability [35]: The vehicle maintains the desired spacing from the adjacent vehicles, and achieves the synchronization of velocity and acceleration with the leader within a fixed time.
- String stability [36]: e_i does not amplify along the vehicle platoon, that is

$$\left|\frac{E_{i+1}(s)}{E_i(s)}\right| \le 1,\ \ i = 1, 2, \ldots, N \tag{12}$$

where $E_i(s)$ represents the Laplace transform of e_i.
- Prescribed tracking performance [37]: The vehicle platoon achieves predefined tracking performance, i.e., $\rho_{i,l} < e_i < \rho_{i,r}$.

Remark 1: One of the objectives in this paper is to ensure that e_i evolves within the range defined by performance boundaries and ultimately converges to a neighborhood of zero, i.e., for $t \ge 0$, $\rho_{i,l}(t) < e_i(t) < \rho_{i,r}(t)$. Therefore, when $t = 0$, the selected parameters should ensure that $e_i(0)$ is within the performance boundaries. As t tends to infinity, the chosen parameters should ensure that the performance boundaries approach zero. Specifically, $\rho_{i,l}(\infty)$ and $\rho_{i,r}(\infty)$ are small constants and satisfy the conditions that $\rho_{i,l}(\infty) < 0$ and $\rho_{i,r}(\infty) > 0$.

Remark 2: According to (5) and Figure. 2, we can conclude that the performance boundaries of traditional PPF are conservative and the convergence time cannot be predefined, which is detrimental to enhancing system performance. Therefore,

This article has been accepted for publication in IEEE Access. This is the author's version which has not been fully edited and content may change prior to final publication. Citation information: DOI 10.1109/ACCESS.2025.3535827

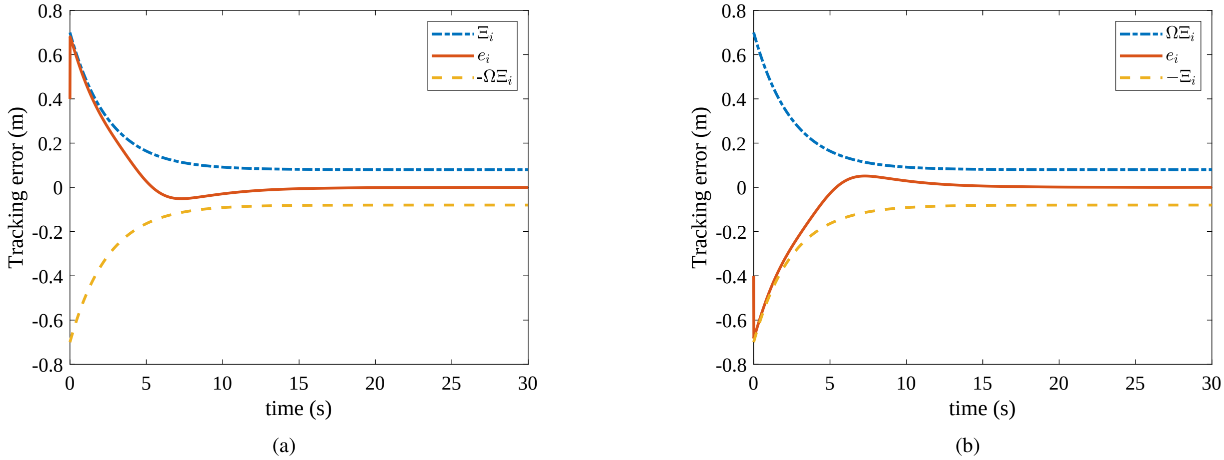

FIGURE 2: e_i under traditional PPC. (a) $e_i(0) \geq 0$. (b) $e_i(0) < 0$.

the TFTPPF is developed, which features more compact performance boundaries and allows for preset convergence time, thereby reducing tracking error overshoot, improving convergence speed, and enabling better transient and steady-state performance for vehicle platoon.

Before designing the controller, we introduce in advance some useful lemmas.

Lemma 1: [38] Consider the following system

$$\dot{x} = -\alpha sig^{\frac{\bar{\lambda}_1}{\bar{\lambda}_2}}(x) - \beta sig^{\frac{\bar{h}_1}{\bar{h}_2}}(x) \tag{13}$$

where $\alpha > 0$, $\beta > 0$; $\bar{\lambda}_1$, $\bar{\lambda}_2$, $\bar{h}_1$, $\bar{h}_2$ satisfy $\bar{\lambda}_1 > \bar{\lambda}_2 > 0$, $\bar{h}_2 > \bar{h}_1 > 0$; $sig^{\Im}(x) = |x|^{\Im} sign(x)$ with $\Im > 0$.

Then, (13) is fixed-time stable (FTS) and the convergence time

$$T_1 \leq \bar{T}_1 = \frac{1}{\alpha}\frac{\bar{\lambda}_2}{\bar{\lambda}_1 - \bar{\lambda}_2} + \frac{1}{\beta}\frac{\bar{h}_1}{\bar{h}_1 - \bar{h}_2} \tag{14}$$

Lemma 2: [22] For $\tau \in R$ and $\forall \mu \geq 0$, the following inequality holds

$$0 \leq |\mu| - \mu \tanh(\frac{\mu}{\tau}) \leq \kappa\tau \tag{15}$$

where $\kappa = 0.2785$.

Lemma 3: [39] Consider $\tau_1, \tau_2, \ldots, \tau_H > 0$, then

$$\begin{aligned} \sum_{i=1}^{H} \tau_i^y &\geq \Big(\sum_{i=1}^{H} \tau_i\Big)^y, \ 0 < y \leq 1 \\ \sum_{i=1}^{H} \tau_i^y &\geq H^{1-y}\Big(\sum_{i=1}^{H} \tau_i\Big)^y, \ 1 < y < \infty \end{aligned} \tag{16}$$

where $y > 0$.

Lemma 4: [40] If there is a Lyapunov function $V(x)$ satisfies

$$\dot{V}(x) \leq -\chi V^{o_1}(x) - \eta V^{o_2}(x) + \sigma \tag{17}$$

where $o_1 > 1$, $0 < o_2 < 1$, $\chi > 0$, $\eta > 0$, and $\sigma > 0$.

Then, the system is FTS and the convergence time T_2 satisfies

$$T_2 \leq \bar{T}_2 = \frac{1}{\chi(o_1 - 1)U} + \frac{1}{\eta(1 - o_2)U} \tag{18}$$

where $0 < U < 1$.

Lemma 5: [33] The following inequality holds

$$p_1 p_2 \leq \frac{\vartheta^{g_1}}{g_1}|p_1|^{L_1} + \frac{1}{L_2\vartheta^{L_2}}|p_2|^{L_2} \tag{19}$$

where $\vartheta > 0$, $p_1 > 0$, $p_2 > 0$, $g_1 > 1$, $g_2 > 1$, and $(g_1 - 1)(g_2 - 1) = 1$.

Lemma 6: [41] The CNN is a functional connectivity network based on Chebyshev polynomials (CP), which has been proven capable of approximating nonlinear systems. Therefore, for a continuous nonlinear function $f(Z)$: $\Re^n \to \Re, f(Z)$ can be described by CNN as

$$f(Z) = W^*\zeta(Z) + \varepsilon \tag{20}$$

where $Z \in \Re^n$ denotes the input vector; ε is approximation error; $W^* \in \Re^{1\times(nM_1+1)}$ represents the optimal weight vector with M_1 being the order of CP; $\zeta(Z) \in \Re^{(nM_1+1)\times 1}$ denotes basis function, which is described as

$$\zeta(Z) = [1, \zeta_1(z_1), \ldots, \zeta_{M_1}(z_1), \ldots, \zeta_1(z_n), \ldots, \zeta_{M_1}(z_n)]^T$$

where $\zeta_k(z_j)$ $(k = 1, \ldots, M_1; j = 1, \ldots, n)$ can be derived through the following two-term recursive formula

$$\begin{aligned} \zeta_{k+1}(z_j) &= 2z_j\zeta_k(z_j) - \zeta_{k-1}(z_j) \\ \zeta_0(z_j) &= 1, \zeta_1(z_j) = z_j, z_j \in \Re \end{aligned}$$

Lemma 7: [42] The following inequality holds

$$\begin{aligned} G(M-G)^y &\leq \frac{y}{y+1}\Big(G^{y+1} - M^{y+1}\Big), \ y \geq 1 \\ G(M-G)^{y+1} &\leq \frac{y+1}{y+2}\Big(G^{y+2} - M^{y+1}\Big), \ 0 < y < 1 \end{aligned} \tag{21}$$

where $G \geq M \geq 0$, and $y > 0$.

This article has been accepted for publication in IEEE Access. This is the author's version which has not been fully edited and content may change prior to final publication. Citation information: DOI 10.1109/ACCESS.2025.3535827

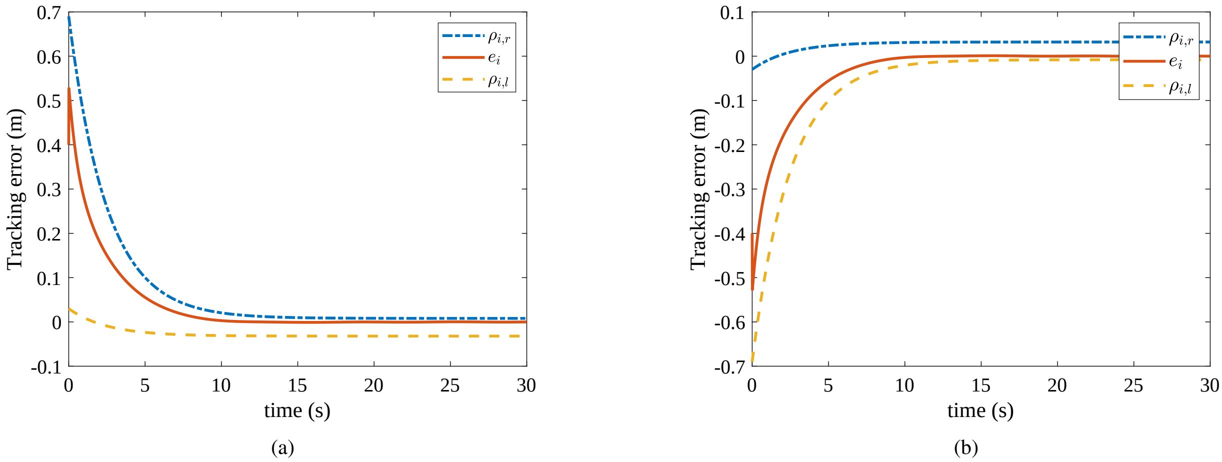

FIGURE 3: e_i under TFTPPF. (a) $e_i(0) \geq 0$. (b) $e_i(0) < 0$.

III. CONTROLLER DESIGN AND STABILITY ANALYSIS

In this section, the vehicle platoon strategy is designed to achieve aforementioned objectives. Before controller design, (2) is converted into a input-related function as

$$Dz_i(u_i) = z_i u_i + \gamma_i \tag{22}$$

where

$$z_i = \begin{cases} z_{i,r} u_i \geq 0 \\ z_{i,l} u_i < 0 \end{cases} \quad \text{and} \quad \gamma_i = \begin{cases} -z_{i,r}\gamma_{i,r}, & u_i \geq \gamma_{i,r} \\ -z_i u_i, & -\gamma_{i,l} < u_i < \gamma_{i,r} \\ z_{i,l}\gamma_{i,l}, & u_i \leq -\gamma_{i,l}. \end{cases}$$

According to (22), we can obtain

$$|\gamma_i| \leq \bar{\gamma}_i \tag{23}$$

where $\bar{\gamma}_i = \max\{|z_{i,r}\gamma_{i,r}|, |z_{i,l}\gamma_{i,l}|\}$.

Define a sliding mode surface as

$$s_i = \dot{\omega}_i + \alpha_1 sig^{\frac{\bar{m}_1}{\bar{n}_1}}(\omega_i) + \alpha_2 sig^{\frac{\bar{m}_2}{\bar{n}_2}}(\omega_i) \tag{24}$$

where $\alpha_1 > 0$, $\alpha_2 > 0$, $\bar{m}_1 > \bar{n}_1 > 0$, and $\bar{n}_2 > \bar{m}_2 > 0$.

To ensure string stability, a coupled sliding mode surface is developed as

$$S_i = \begin{cases} q s_i - s_{i+1}, & i = 1, \dots, N-1 \\ q s_i, & i = N \end{cases} \tag{25}$$

where $0 < q \leq 1$ is coupled weight factor and $s_{N+1} = 0$.

Then, we have

$$S = Qs \tag{26}$$

where

$$Q = \begin{bmatrix} q & -1 & \cdots & 0 & 0 \\ 0 & q & -1 & \cdots & 0 \\ & & \ddots & & \\ 0 & 0 & \cdots & q & -1 \\ 0 & 0 & \cdots & 0 & q \end{bmatrix}$$

$$s = [s_1 \quad s_2 \quad \cdots \quad s_N]^T$$
$$S = [S_1 \quad S_2 \quad \cdots \quad S_N]^T.$$

Differentiating (26) yields

$$\begin{aligned} \dot{S}_i =& q\dot{s}_i - \dot{s}_{i+1} \\ =& q\Big[\frac{\bar{m}_1}{\bar{n}_1}\alpha_1 sig^{\frac{\bar{m}_1-\bar{n}_1}{\bar{n}_1}}(\omega_i)\dot{\omega}_i + \frac{\bar{m}_2}{\bar{n}_2}\alpha_2 sig^{\frac{\bar{m}_2-\bar{n}_2}{\bar{n}_2}}(\omega_i)\dot{\omega}_i \\ &+ \dot{A}_i(\dot{e}_i + \Pi_i) + A_i(\ddot{e}_i + \dot{\Pi}_i)\Big] - \dot{s}_{i+1} \end{aligned} \tag{27}$$

where $\dot{\omega}_i = A_i[\dot{e}_i + \Pi_i]$, $\Pi_i = \frac{e_{i,l}\dot{e}_{i,r} - \dot{e}_{i,l}e_{i,r} - e_i(\dot{\rho}_{i,r} - \dot{\rho}_{i,l})}{e_{i,r} - e_{i,l}}$, and $A_i = \frac{1}{(1-\theta_i)(\rho_{i,r}-\rho_{i,l})\theta_i} > 0$.

For $i = N$, we have

$$\begin{aligned} \dot{S}_N =& q\dot{s}_N \\ =& q\Big[\frac{\bar{m}_1}{\bar{n}_1}\alpha_1 sig^{\frac{\bar{m}_1-\bar{n}_1}{\bar{n}_1}}(\omega_N)\dot{\omega}_N + \frac{\bar{m}_2}{\bar{n}_2}\alpha_2 sig^{\frac{\bar{m}_2-\bar{n}_2}{\bar{n}_2}}(\omega_N)\dot{\omega}_N \\ &+ \dot{A}_N(\dot{e}_N + \Pi_N) + A_N(\ddot{e}_N + \dot{\Pi}_N)\Big] \end{aligned} \tag{28}$$

Define the reaching law as

$$\dot{S}_i = -\beta_1 sig^{r_1}(S_i) - \beta_2 sig^{l_1}(S_i) \tag{29}$$

where $\beta_1 > 0$, $\beta_2 > 0$, $r_1 > 1$, and $0 < l_1 < 1$.

According to Lemma 6, $f_i(v_i(t), a_i(t))$ can be approximated by CNN as

$$f_i(v_i(t), a_i(t)) = W_i^* \zeta_i(Z_i) + \varepsilon_i \tag{30}$$

where W_i^* denotes the optimal weight vector; $\zeta_i(Z_i)$ denotes basis function; ε_i is approximation error satisfying $|\varepsilon_i| \leq \bar{\varepsilon}_i$ with $\bar{\varepsilon}_i > 0$;

As z_i, ι_i, and ϖ_i are often difficult or even impossible to obtain directly in practice, the adaptive mechanisms are developed to estimate them as

$$\begin{aligned} \dot{\hat{z}}_i =& \upsilon_{zi}(-F_i S_i u_i - k_1 \hat{z}_i^{r_1} - k_2 \hat{z}_i^{l_1+1}) \\ \dot{\hat{\iota}}_i =& \upsilon_{\iota i}\left(F_i S_i \tanh\left(\frac{S_i}{\xi_i}\right) - k_3 \hat{\iota}_i^{r_1} - k_4 \hat{\iota}_i^{l_1+1}\right) \\ \dot{\hat{\varpi}}_i =& \upsilon_{\varpi i}\left(F_i^2 S_i^2 \frac{\vartheta_i^2}{2}\zeta_i^T\zeta_i - k_5 \hat{\varpi}_i^{r_1} - k_6 \hat{\varpi}_i^{l_1+1}\right) \end{aligned} \tag{31}$$

This article has been accepted for publication in IEEE Access. This is the author's version which has not been fully edited and content may change prior to final publication. Citation information: DOI 10.1109/ACCESS.2025.3535827

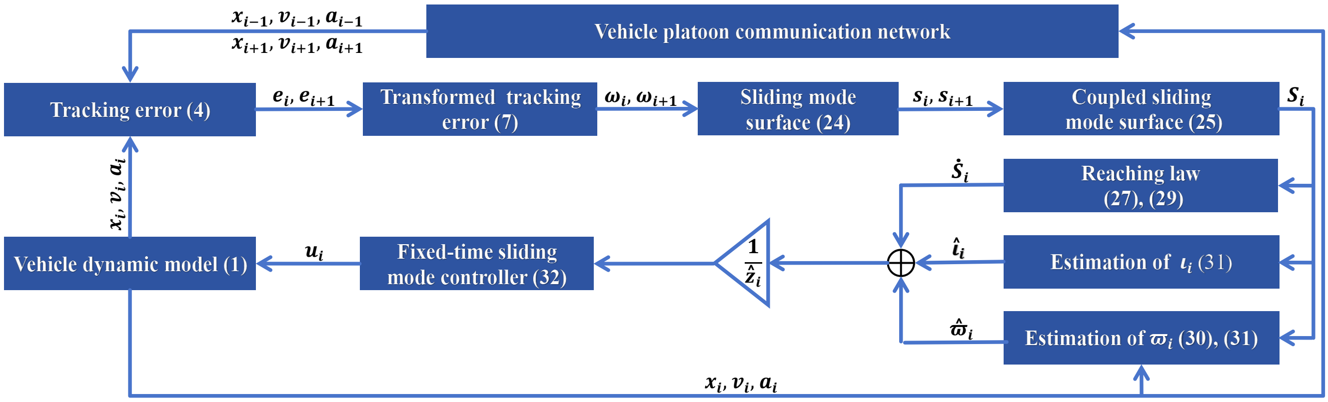

FIGURE 4: The design block diagram of the controller.

where $F_i = qA_i(h_1 + 2h_2 v_i)$, $\varpi_i = \|W_i^*\|^2 = W_i^{*T} W_i^*$, $\iota_i \geq |\bar{D}_i + \bar{\gamma}_i + \bar{\varepsilon}_i|$; ϑ_i, ξ_i, υ_{zi}, $\upsilon_{\iota i}$, and $\upsilon_{\varpi i}$ are positive constants; k_1, k_2, k_3, k_4, k_5, k_6 are small constants.

The novel fixed-time sliding mode controller is designed as

$$
\begin{aligned}
u_i =& \frac{1}{F_i \hat{z}_i}\Big[\beta_1 sig^{r_1}(S_i) + \beta_2 sig^{l_1}(S_i) + F_i^2 S_i \frac{\vartheta_i^2}{2}\hat{\varpi}_i \zeta_i^T \zeta_i \\
&+ F_i \hat{\iota}_i \tanh\left(\frac{S_i}{\xi_i}\right) + Y_i\Big]
\end{aligned} \tag{32}
$$

where

$$
Y_i = \begin{cases}
qA_i(a_{i-1} - a_i - 2h_2 a_i^2) + q(\frac{\bar{m}_1}{\bar{n}_1}\alpha_1 sig^{\frac{\bar{m}_1 - \bar{n}_1}{\bar{n}_1}}(\omega_i)\dot{\omega}_i \\
+\frac{\bar{m}_2}{\bar{n}_2}\alpha_2 sig^{\frac{\bar{m}_2 - \bar{n}_2}{\bar{n}_2}}(\omega_i)\dot{\omega}_i + \dot{A}_i(\dot{e}_i + \Pi_i)) + qA_i\dot{\Pi}_i \\
-\dot{s}_{i+1}, i = 1, \ldots, N-1. \\
qA_i(a_{i-1} - a_i - 2h_2 a_i^2) + q(\frac{\bar{m}_1}{\bar{n}_1}\alpha_1 sig^{\frac{\bar{m}_1 - \bar{n}_1}{\bar{n}_1}}(\omega_i)\dot{\omega}_i \\
+\frac{\bar{m}_2}{\bar{n}_2}\alpha_2 sig^{\frac{\bar{m}_2 - \bar{n}_2}{\bar{n}_2}}(\omega_i)\dot{\omega}_i + \dot{A}_i(\dot{e}_i + \Pi_i)) \\
+qA_i\dot{\Pi}_i, i = N.
\end{cases}
$$

Remark 3: A disadvantage of CNN control method is that the number of parameters to be estimated grows rapidly as the number of nodes increases, potentially resulting in excessive computational load. Inspired by [43], this paper adopts the minimum learning parameter technique, where the number of parameters depends only on the number of vehicles, thereby effectively addressing the aforementioned issue.

Theorem 2: For vehicle platoon (1) with unknown nonlinearities, IDZ, and external disturbances, the adaptive mechanisms (31) and the controller (32) can ensure that e_i converges to a neighborhood of zero within a fixed time, and the individual stability can be guaranteed. Furthermore, if $0 < q \leq 1$ holds, the string stability can be ensured.

To more clearly explain the structure of the controller (32), we present its design block diagram as shown in Figure. 4.

Proof: Define the Lyapunov function as

$$
V_i = \frac{1}{2}S_i^2 + \frac{1}{2\upsilon_{z_i}}\tilde{z}_i^2 + \frac{1}{2\upsilon_{\iota_i}}\tilde{\iota}_i^2 + \frac{1}{2\upsilon_{\varpi_i}}\tilde{\varpi}_i^2 \tag{33}
$$

where $(\tilde{\cdot}) = (\hat{\cdot}) - (\cdot)$. Differentiating (33) yields

$$
\dot{V}_i = S_i\dot{S}_i - \frac{1}{\upsilon_{z_i}}\tilde{z}_i\dot{\hat{z}}_i - \frac{1}{\upsilon_{\iota_i}}\tilde{\iota}_i\dot{\hat{\iota}}_i - \frac{1}{\upsilon_{\varpi_i}}\tilde{\varpi}_i\dot{\hat{\varpi}}_i \tag{34}
$$

According to (27) and (32), one has

$$
\begin{aligned}
S_i\dot{S}_i =& F_i S_i(-z_i u_i - \gamma_i - f_i(v_i, a_i) - D_i) + Y_i S_i \\
=& F_i S_i(-(\hat{z}_i - \tilde{z}_i)u_i - \gamma_i - f_i(v_i, a_i) \\
&- D_i) + Y_i S_i \\
\leq& F_i S_i(-\tilde{z}_i u_i + \bar{\gamma}_i - W_i^{*T}\zeta_i + \bar{\varepsilon}_i + \bar{D}_i) \\
&+ Y_i S_i - (F_i^2 S_i^2 \frac{\vartheta_i^2}{2}\hat{\varpi}_i\zeta_i^T\zeta_i \\
&+ F_i\hat{\iota}_i S_i \tanh(\frac{S_i}{\xi_i}) + Y_i S_i \\
&+ \beta_1 S_i^{r_1+1} + \beta_2 S_i^{l_1+1})
\end{aligned} \tag{35}
$$

Based on Lemma 5, we have

$$
-F_i S_i W_i^{*T}\zeta_i \leq F_i^2 S_i^2 \frac{\vartheta_i^2}{2}\varpi_i\zeta_i^T\zeta_i + \frac{1}{2\vartheta_i^2} \tag{36}
$$

According to (35) and (36), we can obtain

$$
\begin{aligned}
S_i\dot{S}_i \leq& F_i S_i(-\tilde{z}_i u_i + F_i S_i \frac{\vartheta_i^2}{2}\tilde{\varpi}_i\zeta_i^T\zeta_i + \iota_i) \\
&+ \frac{1}{2\vartheta_i^2 S_i F_i} - (F_i\hat{\iota}_i S_i \tanh(\frac{S_i}{\xi_i}) \\
&+ \beta_1 S_i^{r_1+1} + \beta_2 S_i^{l_1+1})
\end{aligned} \tag{37}
$$

By combining (31), (34), and (37), we have

$$
\begin{aligned}
\dot{V}_i \leq& -\beta_1 S_i^{r_1+1} - \beta_2 S_i^{l_1+1} + k_1\tilde{z}_i\hat{z}_i^{r_1} \\
&+ k_2\tilde{z}_i\hat{z}_i^{l_1+1} + k_3\tilde{\iota}_i\hat{\iota}_i^{r_1} + k_4\tilde{\iota}_i\hat{\iota}_i^{l_1+1} \\
&+ k_5\tilde{\varpi}_i\hat{\varpi}_i^{r_1} + k_6\tilde{\varpi}_i\hat{\varpi}_i^{l_1+1} + F_i\iota_i(S_i \\
&- S_i\tanh(\frac{S_i}{\xi_i})) + \frac{1}{2\vartheta_i^2}
\end{aligned} \tag{38}
$$

This article has been accepted for publication in IEEE Access. This is the author's version which has not been fully edited and content may change prior to final publication. Citation information: DOI 10.1109/ACCESS.2025.3535827

Based on Lemma 7, one can obtain

$$\begin{aligned}
k_1\tilde{z}_i\hat{z}_i^{r_1} &= k_1\tilde{z}_i(z_i-\tilde{z}_i)^{r_1} \\
&\le \frac{k_1r_1}{r_1+1}(z_i^{r_1+1}-\tilde{z}_i^{r_1+1}) \\
k_2\tilde{z}_i\hat{z}_i^{l_1+1} &= k_2\tilde{z}_i(z_i-\tilde{z}_i)^{l_1+1} \\
&\le \frac{k_2(l_1+1)}{l_1+2}(z_i^{l_1+2}-\tilde{z}_i^{l_1+1}) \\
k_3\tilde{\iota}_i\hat{\iota}_i^{r_1} &= k_3\tilde{\iota}_i(\iota_i-\tilde{\iota}_i)^{r_1} \\
&\le \frac{k_3r_1}{r_1+1}(\iota_i^{r_1+1}-\tilde{\iota}_i^{r_1+1}) \\
k_4\tilde{\iota}_i\hat{\iota}_i^{l_1+1} &= k_4\tilde{\iota}_i(\iota_i-\tilde{\iota}_i)^{l_1+1} \\
&\le \frac{k_4(l_1+1)}{l_1+2}(\iota_i^{l_1+2}-\tilde{\iota}_i^{l_1+1}) \\
k_5\tilde{\varpi}_i\hat{\varpi}_i^{r_1} &= k_5\tilde{\varpi}_i(\varpi_i-\tilde{\varpi}_i)^{r_1+1} \\
&\le \frac{k_5r_1}{r_1+1}(\varpi_i^{r_1+1}-\tilde{\varpi}_i^{r_1+1}) \\
k_6\tilde{\varpi}_i\hat{\varpi}_i^{l_1+1} &= k_6\tilde{\varpi}_i(\varpi_i-\tilde{\varpi}_i)^{l_1} \\
&\le \frac{k_6(l_1+1)}{l_1+2}(\varpi_i^{l_1+2}-\tilde{\varpi}_i^{l_1+1})
\end{aligned} \tag{39}$$

According to Lemma 2, one has

$$F_i\iota_i\Big(S_i - S_i\tanh(\frac{S_i}{\xi_i})\Big) \le 0.2785F_i\iota_i\xi_i \tag{40}$$

By combining (38), (39), and (40), we can obtain

$$\begin{aligned}
\dot{V}_i \le &-\beta_1 S_i^{r_1+1} - \frac{k_1r_1}{r_1+1}\tilde{z}_i^{r_1+1} - \frac{k_3r_1}{r_1+1}\tilde{\iota}_i^{r_1+1} \\
&- \frac{k_5r_1}{r_1+1}\tilde{\varpi}_i^{r_1+1} - \beta_2 S_i^{l_1+1} - \frac{k_2(l_1+1)}{l_1+2}\tilde{z}_i^{l_1+1} \\
&- \frac{k_4(l_1+1)}{l_1+2}\tilde{\iota}_i^{l_1+1} - \frac{k_6(l_1+1)}{l_1+2}\tilde{\varpi}_i^{l_1+1} + \frac{k_1r_1}{r_1+1}z_i^{r_1+1} \\
&+ \frac{k_2(l_1+1)}{l_1+2}z_i^{l_1+2} + \frac{k_3r_1}{r_1+1}\iota_i^{r_1+1} + \frac{k_4(l_1+1)}{l_1+2}\iota_i^{l_1+2} \\
&+ \frac{k_5r_1}{r_1+1}\varpi_i^{r_1+1} + \frac{k_6(l_1+1)}{l_1+2}\varpi_i^{l_1+2} + \frac{1}{2\vartheta_i^2} \\
&+ F_i\iota_i 0.2785\xi_i \\
\le &-\beta_1(S_i^2)^{\frac{r_1+1}{2}} - \frac{k_1r_1}{r_1+1}(\tilde{z}_i^2)^{\frac{r_1+1}{2}} - \frac{k_3r_1}{r_1+1}(\tilde{\iota}_i^2)^{\frac{r_1+1}{2}} \\
&- \frac{k_5r_1}{r_1+1}(\tilde{\varpi}_i^2)^{\frac{r_1+1}{2}} - \beta_2(S_i^2)^{\frac{l_1+1}{2}} - \frac{k_2(l_1+1)}{l_1+2}(\tilde{z}_i^2)^{\frac{l_1+1}{2}} \\
&- \frac{k_4(l_1+1)}{l_1+2}(\tilde{\iota}_i^2)^{\frac{l_1+1}{2}} - \frac{k_6(l_1+1)}{l_1+2}(\tilde{\varpi}_i^2)^{\frac{l_1+1}{2}} \\
&+ \frac{k_1r_1}{r_1+1}z_i^{r_1+1} + + \frac{k_2(l_1+1)}{l_1+2}z_i^{l_1+2} + \frac{k_3r_1}{r_1+1}\iota_i^{r_1+1} \\
&+ \frac{k_4(l_1+1)}{l_1+2}\iota_i^{l_1+2} + \frac{k_5r_1}{r_1+1}\varpi_i^{r_1+1} + \frac{k_6(l_1+1)}{l_1+2}\varpi_i^{l_1+2} \\
&+ F_i\iota_i 0.2785\xi_i + \frac{1}{2\vartheta_i^2}
\end{aligned} \tag{41}$$

Then, (41) can be rewritten as

$$\begin{aligned}
\dot{V}_i \le& \chi_i\Big((\frac{1}{2}S_i^2)^{\frac{r_1+1}{2}} + (\frac{1}{2\upsilon_{z_i}}\tilde{z}_i^2)^{\frac{r_1+1}{2}} + (\frac{1}{2\upsilon_{\iota_i}}\tilde{\iota}_i^2)^{\frac{r_1+1}{2}} \\
&+ (\frac{1}{2\upsilon_{\varpi_i}}\tilde{\varpi}_i^2)^{\frac{r_1+1}{2}}\Big) + \eta_i\Big((\frac{1}{2}S_i^2)^{\frac{l_1+1}{2}} + (\frac{1}{2\upsilon_{z_i}}\tilde{z}_i^2)^{\frac{l_1+1}{2}} \\
&+ (\frac{1}{2\upsilon_{\iota_i}}\tilde{\iota}_i^2)^{\frac{l_1+1}{2}} + (\frac{1}{2\upsilon_{\varpi_i}}\tilde{\varpi}_i^2)^{\frac{l_1+1}{2}}\Big) + \sigma_i
\end{aligned} \tag{42}$$

where

$$\begin{aligned}
\chi_i =& \min\{2^{\frac{1+r_1}{2}}\beta_1, (2\upsilon_{zi})^{\frac{1+r_1}{2}}\frac{k_1r_1}{r_1+1}, (2\upsilon_{\iota i})^{\frac{1+r_1}{2}}\frac{k_3r_1}{r_1+1}, \\
&(2\upsilon_{\varpi i})^{\frac{1+r_1}{2}}\frac{k_5r_1}{r_1+1}\} \\
\eta_i =& \min\{2^{\frac{1+l_1}{2}}\beta_2, (2\upsilon_{zi})^{\frac{1+l_1}{2}}\frac{k_2(l_1+1)}{l_1+2}, \\
&(2\upsilon_{\iota_i i})^{\frac{1+l_1}{2}}\frac{k_4(l_1+1)}{l_1+2}, (2\upsilon_{\varpi i})^{\frac{1+l_1}{2}}\frac{k_6(l_1+1)}{l_1+2}\} \\
\sigma_i =& \frac{k_1r_1}{r_1+1}z_i^{r_1+1} + \frac{k_2(l_1+1)}{l_1+2}z_i^{l_1+2} + \frac{k_3r_1}{r_1+1}\iota_i^{r_1+1} \\
&+ \frac{k_4(l_1+1)}{l_1+2}\iota_i^{l_1+2} + \frac{k_5r_1}{r_1+1}\varpi_i^{r_1+1} \\
&+ \frac{k_6(l_1+1)}{l_1+2}\varpi_i^{l_1+2} + F_i\iota_i 0.2785\xi_i + \frac{1}{2\vartheta_i^2}.
\end{aligned}$$

According to Lemma 3, we have

$$V \le -\chi_i 4^{\frac{1-r_1}{2}}V_i^{\frac{r_1+1}{2}} - \eta_i V_i^{\frac{l_1+1}{2}} + \sigma_i \tag{43}$$

By Lemma 4, we can obtain that V_i is FTS. It means that S_i, $\tilde{z}_i$, $\tilde{\iota}_i$, and $\tilde{\varpi}_i$ can converge to a neighborhood of zero within convergence time $T_{i,1}$. $T_{i,1}$ is given as

$$T_{i,1} \le \bar{T}_{i,1} = \frac{1}{\chi_i 4^{\frac{1-r_1}{2}}(\frac{r_1-1}{2})M_i} + \frac{1}{\eta_i(\frac{1-l_1}{2})M_i} \tag{44}$$

where $0 < M_i < 1$.

Based on (7), (24), (25), and Lemma 1, s_i, ω_i, and e_i can converge to a neighborhood of zero within convergence time $T_{i,2}$ when $S_i = 0$. $T_{i,2}$ is described as

$$T_{i,2} \le \bar{T}_{i,2} = \frac{1}{\alpha_1}\frac{\bar{n}_1}{\bar{m}_1 - \bar{n}_1} + \frac{1}{\alpha_2}\frac{\bar{n}_2}{\bar{n}_2 - \bar{m}_2} \tag{45}$$

According to (44) and (45), the maximum value of the convergence time as

$$T_{i,max} = T_{i,1} + T_{i,2} \tag{46}$$

It means that the vehicle platoon (1) can achieve the individual stability within $T_{i,max}$. The proof of string stability is similar to the proof process in [34]. As $S_i = qs_i - s_{i+1}$, when S_i converges to a neighborhood of zero, we have

$$\begin{aligned}
&q\Big[\dot{\omega}_i + \alpha_1 sig^{\frac{\bar{m}_1}{\bar{n}_1}}(\omega_i) + \alpha_2 sig^{\frac{\bar{m}_2}{\bar{n}_2}}(\omega_i)\Big] \\
&\approx \Big[\dot{\omega}_{i+1} + \alpha_1 sig^{\frac{\bar{m}_1}{\bar{n}_1}}(\omega_{i+1}) + \alpha_2 sig^{\frac{\bar{m}_2}{\bar{n}_2}}(\omega_{i+1})\Big]
\end{aligned} \tag{47}$$

By taking the Laplace transform of equation (47), we can get the following two cases.

This article has been accepted for publication in IEEE Access. This is the author's version which has not been fully edited and content may change prior to final publication. Citation information: DOI 10.1109/ACCESS.2025.3535827

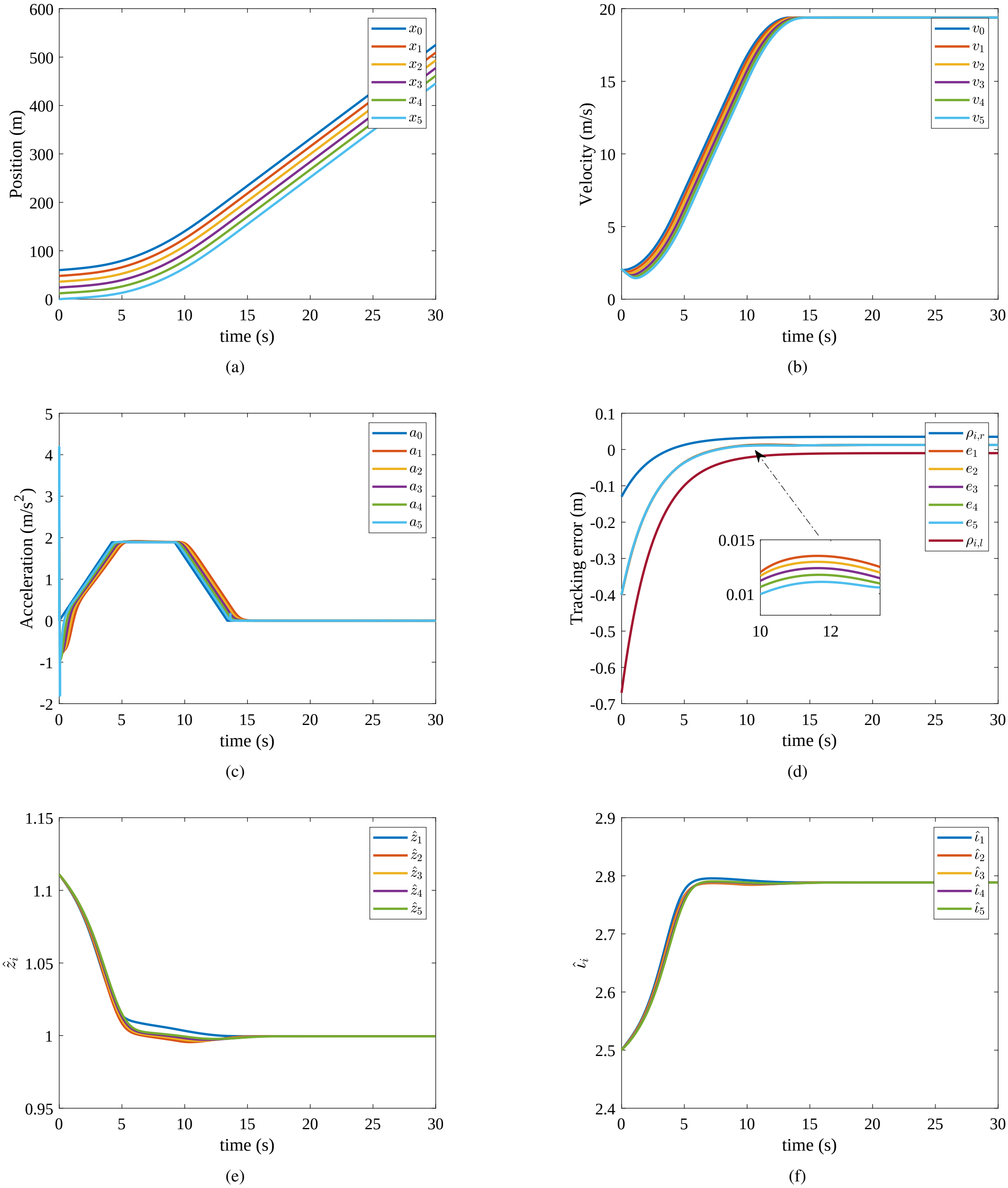

FIGURE 5: The results of the controller with TFTPPF. (a) Position x_i. (b) Velocity v_i. (c) Acceleration a_i. (d) Tracking error e_i. (e) Estimation of z_i. (f) Estimation of ι.

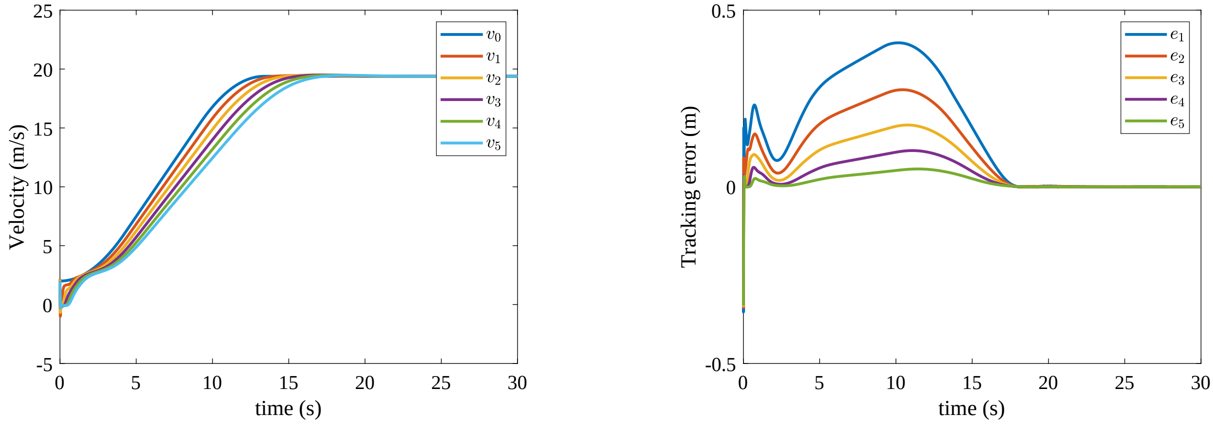

(a) (b)

FIGURE 6: The results of the controller without PPF. (a) Velocity v_i. (b) Tracking error e_i.

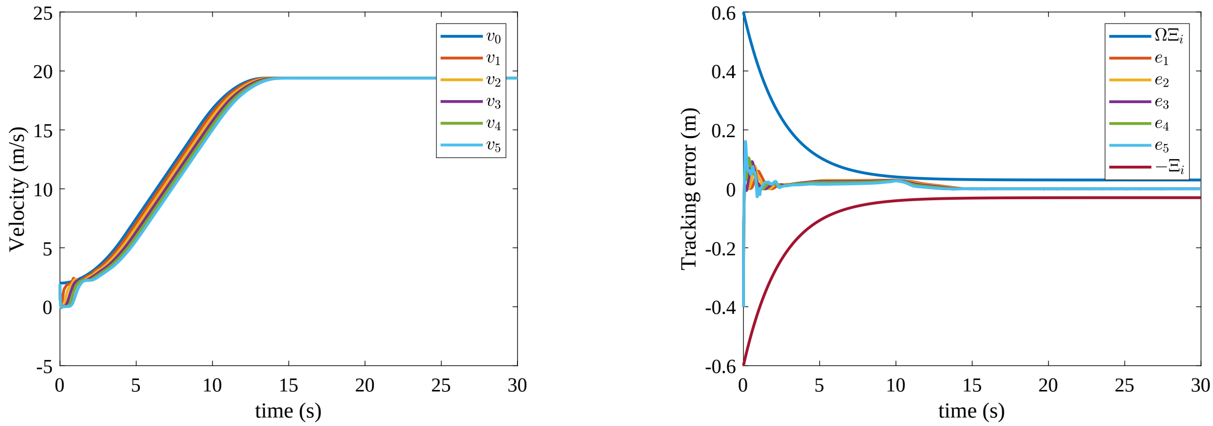

(a) (b)

FIGURE 7: The results of the controller with traditional PPF. (a) Velocity v_i. (b) Tracking error e_i.

Case 1: if $\omega_i \geq 0$, we have

$$q\left[s\bar{W}_i(s)+\alpha_1\bar{W}_i^{\frac{\bar{m}_1}{\bar{n}_1}}(s)+\alpha_2\bar{W}_i^{\frac{\bar{m}_2}{\bar{n}_2}}(s)\right] \approx s\bar{W}_{i+1}(s)+\alpha_1\bar{W}_{i+1}^{\frac{\bar{m}_1}{\bar{n}_1}}(s)+\alpha_2\bar{W}_{i+1}^{\frac{\bar{m}_2}{\bar{n}_2}}(s) \tag{48}$$

Then

$$\frac{\bar{W}_{i+1}(s)}{\bar{W}_i(s)} \approx \frac{q\left[s+\alpha_1\bar{W}_i^{\frac{\bar{m}_1}{\bar{n}_1}-1}(s)+\alpha_2\bar{W}_i^{\frac{\bar{m}_2}{\bar{n}_2}-1}(s)\right]}{s+\alpha_1\bar{W}_{i+1}^{\frac{\bar{m}_1}{\bar{n}_1}-1}(s)+\alpha_2\bar{W}_{i+1}^{\frac{\bar{m}_2}{\bar{n}_2}-1}(s)} \approx q \tag{49}$$

Case 2: if $\omega_i < 0$, we can obtain

$$q\left[s\bar{W}_i(s)-\alpha_1\bar{W}_i^{\frac{\bar{m}_1}{\bar{n}_1}}(s)-\alpha_2\bar{W}_i^{\frac{\bar{m}_2}{\bar{n}_2}}(s)\right] \approx s\bar{W}_{i+1}(s)-\alpha_1\bar{W}_{i+1}^{\frac{\bar{m}_1}{\bar{n}_1}}(s)-\alpha_2\bar{W}_{i+1}^{\frac{\bar{m}_2}{\bar{n}_2}}(s) \tag{50}$$

Then

$$\frac{\bar{W}_{i+1}(s)}{\bar{W}_i(s)} \approx \frac{q\left[s-\alpha_1\bar{W}_i^{\frac{\bar{m}_1}{\bar{n}_1}-1}(s)-\alpha_2\bar{W}_i^{\frac{\bar{m}_2}{\bar{n}_2}-1}(s)\right]}{s-\alpha_1\bar{W}_{i+1}^{\frac{\bar{m}_1}{\bar{n}_1}-1}(s)-\alpha_2\bar{W}_{i+1}^{\frac{\bar{m}_2}{\bar{n}_2}-1}(s)} \approx q \tag{51}$$

where $\bar{W}_i(s)$ is the Laplace transform of ω_i. According to (7), ω_i and e_i have the same monotonicity. Therefore, when $0 < q \leq 1$, string stability can be guaranteed. The proof is completed.

IV. NUMERICAL EXAMPLES

In this section, we will illustrate the effectiveness and advantages of the proposed strategy through numerical examples.

Consider a vehicle platoon consisting of one leader and five following vehicles. The parameters of vehicle platoon are the same as those in [15]: the air density $\rho_a = 0.2$, the mass $m_i = [1500, 1600, 1550, 1650, 1600]$, the engine time constant $\tau_i =$

$[0.15, 0.3, 0.2, 0.25, 0.2]$, the angle of the road slope $\phi = 0$, the rolling resistance coefficient $\ell_i = 0.1$, the cross-sectional area $A_i = 2.2$, the acceleration of the gravity $g = 9.8$, the air drag coefficient $C_{di} = 0.35$, $h_1 = 0.2$, $h_2 = 10^{-5}$, the external disturbances $D_i = 0.1\sin(t)$, the length of vehicle $w_i = 2$, and the standstill spacing $\mu_i = 10$.

A. RESULTS OF DESIGNED CONTROLLER STRATEGY

In this subsection, using the adaptive mechanisms (31) and the controller (32), numerical examples are carried out to verify the effectiveness of the proposed strategy. The parameters of the controller are $z_{i,r} = 1$, $z_{i,l} = 0.95$, $\gamma_{i,r} = 2$,$\gamma_{i,l} = 1.9$, $\vartheta_i = 0.1$, $\delta_{i,0} = 0.6$, $\delta_{i,\infty} = 0.05$, $\varphi_i = 0.4$, $t_f = 20$, $\kappa_1 = 0.9$, $\kappa_2 = 1.2$, $\varsigma_1 = 0.3$, $\varsigma_2 = 0.9$, $\xi_i = 0.1$, $\upsilon_{zi} = \upsilon_{\iota i} = \upsilon_{\varpi i} = 0.01$, $k_1 = k_2 = k_3 = k_4 = k_5 = k_6 = 0.001$ and $q = 0.9$.

The results are presented in Figure. 5. The position profiles are presented in Figure. 5(a). As there are no intersections or overlaps, it is indicated that the designed strategy for vehicle platoon can ensure no collision between vehicles. Figure. 5(b) shows that vehicle platoon achieves synchronization of velocity. According to Figure. 5(c), we can obtain that the acceleration of the following vehicle can track the acceleration of the leader. It is evident from Figure. 5(d) that before time t_f, e_i converges to a neighborhood of zero, indicating that the designed strategy can ensure the vehicle platoon maintains the desired spacing. In addition, as e_i consistently remains within the predefined region, we can conclude that the designed strategy can ensure the vehicle platoon achieves the prescribed tracking performance. Figures. 5(e) and (f) demonstrate that the designed adaptive mechanisms can effectively estimate z_i and ι_i.

B. RESULTS OF COMPARATIVE NUMERICAL EXAMPLE

In this subsection, we present two comparative numerical examples to demonstrate the advantages of the designed strategy. The controller parameters are the same as in example 1.

Case:1 Comparison with the control strategy without PPF.

The results are presented in Figure. 6. Figure. 6(a) shows that the velocity of the following vehicle can track the velocity of the leader. It is evident from Figure. 6(b) that e_i can eventually converge to the neighborhood of zero. By comparing Figure. 5 with Figure. 6, we can obtain that the designed strategy can accelerate the convergence rate, reduce the overshoot of e_i, and decreases the velocity fluctuation, thereby enabling the vehicle platoon to possess better transient and steady-state performance.

Case:2 Comparison with the control strategy with traditional PPF. The traditional PPF is selected as [9]: $\Xi_i = (\Xi_{i,0} - \Xi_{i,\infty})e^{-\partial_i t} + \Xi_{i,\infty}$, where $\Xi_{i,0} = 0.6$, $\Xi_{i,\infty} = 0.05$, and $\partial_i = 0.5$.

The results are shown in Figure. 7. By comparing Figure. 5 with Figure. 7, we can see that the designed strategy can effective reduce the overshoot of e_i and decreases the velocity fluctuation. Therefore, the designed strategy can better improve performance of vehicle platoon.

V. CONCLUSION

A FTSMC problem for vehicle platoon with prescribed performance, IDZ, unknown nonlinearities, and external disturbances is investigated. Compared with the traditional funnel-shaped PPF, the designed TFTPPF defines tunnel-shaped performance boundaries that can enhance the convergence rate of e_i and reduce the system overshoot. The convergence time of TFTPPF can be predetermined and is not affected by the initial conditions. CNN is applied to approximate nonlinearities in vehicle platoon, while the novel adaptive mechanisms are designed to estimate IDZ slope and external disturbances. Based on the proposed TFTPPF, CNN, and adaptive mechanisms, a new FTSMC strategy is proposed to ensure string stability and achieve predefined tracking performance within a fixed time. The results of the comparative numerical examples demonstrate that the proposed strategy can effectively reduce overshoot of e_i, accelerate convergence rate, and thus improve system performance. Our future work will be dedicated to researching the control issues of the vehicle platoon with prescribed performance and system failures.

REFERENCES

[1] X. Li, P. Shi, Y. Wang, and S. Wang, "Cooperative tracking control of heterogeneous mixed-order multiagent systems with higher-order nonlinear dynamics," *IEEE Transactions on Cybernetics*, vol. 52, no. 6, pp. 5498–5507, 2020.

[2] Z. Shen, Y. Liu, Z. Li, and Y. Wu, "Distributed vehicular platoon control considering communication delays and packet dropouts," *Journal of the Franklin Institute*, vol. 361, no. 7, p. 106703, 2024.

[3] Y. Liu, D. Yao, L. Wang, and S. Lu, "Distributed adaptive fixed-time robust platoon control for fully heterogeneous vehicles," *IEEE Transactions on Systems, Man, and Cybernetics: Systems*, vol. 53, no. 1, pp. 264–274, 2022.

[4] Y. Wang, H. Dong, and X. Li, "Distributed cooperative neural control for nonlinear heterogeneous platoon systems with unknown uncertainties," *Arabian Journal for Science and Engineering*, pp. 1–14, 2024.

[5] Y. Wang, P. Shi, and X. Li, "Event-triggered observation-based control of nonlinear mixed-order multiagent systems under input saturation," *IEEE Systems Journal*, vol. 18, no. 2, pp. 1392–1401, 2024.

[6] Z. Yao, Y. Ma, T. Ren, and Y. Jiang, "Impact of the heterogeneity and platoon size of connected vehicles on the capacity of mixed traffic flow," *Applied Mathematical Modelling*, vol. 125, pp. 367–389, 2024.

[7] X. Li, P. Shi, and Y. Wang, "Distributed cooperative adaptive tracking control for heterogeneous systems with hybrid nonlinear dynamics," *Nonlinear Dynamics*, vol. 95, pp. 2131–2141, 2019.

[8] H. Li, Z. Chen, B. Fu, and M. Sun, "Nonlinear control of heterogeneous vehicle platoon with time-varying delays and limited communication range," *International Journal of Control, Automation and Systems*, vol. 21, no. 6, pp. 1727–1738, 2023.

[9] Z. Shen, Y. Liu, Z. Li, and M. H. Nabin, "Cooperative spacing sampled control of vehicle platoon considering undirected topology and analog fading networks," *IEEE Transactions on Intelligent Transportation Systems*, vol. 23, no. 10, pp. 18 478–18 491, 2022.

[10] Z. Qiang, L. Dai, B. Chen, and Y. Xia, "Distributed model predictive control for heterogeneous vehicle platoon with inter-vehicular spacing constraints," *IEEE Transactions on Intelligent Transportation Systems*, vol. 24, no. 3, pp. 3339–3351, 2022.

[11] Y. Wang, Y. Liu, X. Li, and Y. Liang, "Distributed consensus tracking control based on state and disturbance observations for mixed-order multiagent mechanical systems," *Journal of the Franklin Institute*, vol. 360, no. 2, pp. 943–963, 2023.

[12] Y. Li, Q. Lv, H. Zhu, H. Li, H. Li, S. Hu, S. Yu, and Y. Wang, "Variable time headway policy based platoon control for heterogeneous connected vehicles with external disturbances," *IEEE Transactions on Intelligent Transportation Systems*, vol. 23, no. 11, pp. 21 190–21 200, 2022.

[13] Z. Gao, Y. Zhang, and G. Guo, "Prescribed-time control of vehicular platoons based on a disturbance observer," *IEEE Transactions on Circuits and Systems II: Express Briefs*, vol. 69, no. 9, pp. 3789–3793, 2022.

[14] W. Wang, J. Liang, C. Pan, Y. Cai, and L. Chen, "Nls based hierarchical anti-disturbance controller for vehicle platoons with time-varying parameter uncertainties," *IEEE Transactions on Intelligent Transportation Systems*, vol. 23, no. 11, pp. 21 062–21 073, 2022.

[15] M. Shen, Y. Gu, Q.-G. Wang, Z.-G. Wu, and J. H. Park, "Tighter interval estimation for discrete-time linear systems with a new dynamic triggering approach," *IEEE Transactions on Instrumentation and Measurement*, vol. 72, pp. 1–11, 2023.

[16] M. Shen, Y. Ma, J. H. Park, and Q.-G. Wang, "Fuzzy tracking control for markov jump systems with mismatched faults by iterative proportional-integral observers," *IEEE Transactions on Fuzzy Systems*, vol. 30, no. 2, pp. 542–554, 2020.

[17] M. Shen, H. Zhang, S. K. Nguang, and C. K. Ahn, "h_∞ output anti-disturbance control of stochastic markov jump systems with multiple disturbances," *IEEE Transactions on Systems, Man, and Cybernetics: Systems*, vol. 51, no. 12, pp. 7633–7643, 2020.

[18] M. Farbood, M. Shasadeghi, T. Niknam, B. Safarinejadian, and A. Izadian, "Cooperative h_∞ robust move blocking fuzzy model predictive control of nonlinear systems," *IEEE Transactions on Systems, Man, and Cybernetics: Systems*, vol. 53, no. 12, pp. 7707–7718, 2023.

[19] M. Farbood, Z. Echreshavi, M. Shasadeghi, and S. Mobayen, "Asynchronous robust fuzzy event-triggered control of nonlinear systems," *Journal of the Franklin Institute*, vol. 360, no. 13, pp. 9904–9923, 2023.

[20] M. Farbood, Z. Echreshavi, M. Shasadeghi, S. Mobayen, and P. Skruch, "Disturbance observer-based data driven model predictive tracking control of linear systems," *IEEE Access*, vol. 11, pp. 88 597–88 608, 2023.

[21] J.-W. Kwon and D. Chwa, "Adaptive bidirectional platoon control using a coupled sliding mode control method," *IEEE Transactions on Intelligent Transportation Systems*, vol. 15, no. 5, pp. 2040–2048, 2014.

[22] X. Guo, J. Wang, F. Liao, and R. S. H. Teo, "Distributed adaptive integrated-sliding-mode controller synthesis for string stability of vehicle platoons," *IEEE Transactions on Intelligent Transportation Systems*, vol. 17, no. 9, pp. 2419–2429, 2016.

[23] Y. Li, C. Tang, K. Li, S. Peeta, X. He, and Y. Wang, "Nonlinear finite-time consensus-based connected vehicle platoon control under fixed and switching communication topologies," *Transportation Research Part C: Emerging Technologies*, vol. 93, pp. 525–543, 2018.

[24] J. Han, J. Zhang, C. He, C. Lv, C. Li, X. Hou, and Y. Ji, "Adaptive distributed finite-time fault-tolerant controller for cooperative braking of the vehicle platoon," *IET Intelligent Transport Systems*, vol. 15, no. 12, pp. 1562–1581, 2021.

[25] S. Yue, B. Niu, H. Wang, L. Zhang, and A. M. Ahmad, "Hierarchical sliding mode-based adaptive fuzzy control for uncertain switched under-actuated nonlinear systems with input saturation and dead-zone," *Robotic Intelligence and Automation*, vol. 43, no. 5, pp. 523–536, 2023.

[26] X. Wang and D. Ye, "Finite-time output-feedback formation control for high-order nonlinear multiagent systems with obstacle avoidance," *IEEE Transactions on Automation Science and Engineering*, vol. 21, no. 2, pp. 1878–1888, 2023.

[27] Y. Liu, R. Chi, H. Li, L. Wang, and N. Lin, "Hitl-based adaptive fuzzy tracking control of mass: A distributed fixed-time strategy," *Science China Technological Sciences*, vol. 66, no. 10, pp. 2907–2916, 2023.

[28] X.-S. Wang, C.-Y. Su, and H. Hong, "Robust adaptive control of a class of nonlinear systems with unknown dead-zone," *Automatica*, vol. 40, no. 3, pp. 407–413, 2004.

[29] G. Sun, X. Ren, Q. Chen, and D. Li, "A modified dynamic surface approach for control of nonlinear systems with unknown input dead zone," *International Journal of Robust and Nonlinear Control*, vol. 25, no. 8, pp. 1145–1167, 2015.

[30] D. Li and G. Guo, "Prescribed performance concurrent control of connected vehicles with nonlinear third-order dynamics," *IEEE Transactions on Vehicular Technology*, vol. 69, no. 12, pp. 14 793–14 802, 2020.

[31] O. Elhaki and K. Shojaei, "Neural network-based target tracking control of underactuated autonomous underwater vehicles with a prescribed performance," *Ocean Engineering*, vol. 167, pp. 239–256, 2018.

[32] Y. Huang, J. Na, X. Wu, X. Liu, and Y. Guo, "Adaptive control of nonlinear uncertain active suspension systems with prescribed performance," *ISA transactions*, vol. 54, pp. 145–155, 2015.

[33] H. Sun, G. Zong, J. Cui, and K. Shi, "Fixed-time sliding mode output feedback tracking control for autonomous underwater vehicle with prescribed performance constraint," *Ocean Engineering*, vol. 247, p. 110673, 2022.

[34] G. Guo and D. Li, "Adaptive sliding mode control of vehicular platoons with prescribed tracking performance," *IEEE Transactions on Vehicular Technology*, vol. 68, no. 8, pp. 7511–7520, 2019.

[35] M. Hu, X. Wang, Y. Bian, D. Cao, and H. Wang, "Disturbance observer-based cooperative control of vehicle platoons subject to mismatched disturbance," *IEEE Transactions on Intelligent Vehicles*, vol. 8, no. 4, pp. 2748–2758, 2023.

[36] X. Guo, J. Wang, F. Liao, and R. S. H. Teo, "Distributed adaptive integrated-sliding-mode controller synthesis for string stability of vehicle platoons," *IEEE Transactions on Intelligent Transportation Systems*, vol. 17, no. 9, pp. 2419–2429, 2016.

[37] K. Shojaei and M. R. Yousefi, "Tracking control of a convoy of autonomous robotic cars with a prescribed performance," *Transactions of the Institute of Measurement and Control*, vol. 41, no. 13, pp. 3725–3741, 2019.

[38] M. Khodaverdian and M. Malekzadeh, "Fixed-time constrained model predictive sliding mode control of spacecraft simulator," *IEEE Transactions on Industrial Electronics*, vol. 70, no. 3, pp. 2739–2747, 2022.

[39] Y. Sun, F. Wang, Z. Liu, Y. Zhang, and C. P. Chen, "Fixed-time fuzzy control for a class of nonlinear systems," *IEEE Transactions on Cybernetics*, vol. 52, no. 5, pp. 3880–3887, 2020.

[40] Z. Gao and G. Guo, "Fixed-time sliding mode formation control of auvs based on a disturbance observer," *IEEE/CAA Journal of Automatica Sinica*, vol. 7, no. 2, pp. 539–545, 2020.

[41] X.-G. Guo, J.-L. Wang, F. Liao, and R. S. H. Teo, "Cnn-based distributed adaptive control for vehicle-following platoon with input saturation," *IEEE Transactions on Intelligent Transportation Systems*, vol. 19, no. 10, pp. 3121–3132, 2017.

[42] Z. Zuo, "Nonsingular fixed-time consensus tracking for second-order multi-agent networks," *Automatica*, vol. 54, pp. 305–309, 2015.

[43] J. Qin and J. Du, "Minimum-learning-parameter-based adaptive finite-time trajectory tracking event-triggered control for underactuated surface vessels with parametric uncertainties," *Ocean Engineering*, vol. 271, p. 113634, 2023.

YIGUANG WANG received the B.S. degree in automation and the M.S. degree in control theory and control engineering from Harbin Engineering University, Harbin, China, in 2003 and 2008, respectively, and the Ph.D. degree in control science and engineering from Harbin Institute of Technology, Harbin, in 2015.

From 2019 to 2020, he was a Postdoctoral Fellow with the Department of Mechanical Engineering, McMaster University, Hamilton, Canada. He is currently an Associate Professor with the College of Mechanical and Control Engineering, Guilin University of Technology, Guilin, China. His current research interests include precision motion control systems, intelligent fault-tolerant control, vehicle platoon control, and networked multiagent systems.

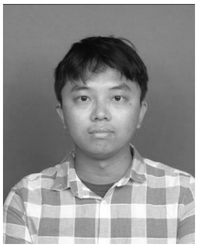

YONGQIANG JIANG received the B.S. degree in automation from Guangxi University of Science and Technology, Liuzhou, China, in 2022. He is currently pursuing the master's degree with the College of Mechanical and Control Engineering, Guilin University of Technology, Guilin, China. His research interests include vehicle platoon control and prescribed performance control.

XIAOJIE LI received the B.S. degree in measurement and control technology and instruments from Heilongjiang University of Science and Technology, Harbin, China, in 2008, and the M.S. degree in detection technology and automatic equipment and the Ph.D. degree in control science and engineering from Harbin Engineering University, Harbin, in 2014 and 2021, respectively.

From 2019 to 2020, she was a Visiting Ph.D. Student with the Department of Mechanical Engineering, McMaster University, Hamilton, Canada. She is currently a Lecturer with the College of Mechanical and Control Engineering, Guilin University of Technology, Guilin, China. Her research interests include multiagent systems, fault-tolerant control, event-triggered control, vehicle platoon control and nonlinear control theory.

XIAOYAN ZHAN received the B.S. degree in automation from Guilin University of Technology, Guilin, China, in 2022. She is currently pursuing the master's degree with the College of Mechanical and Control Engineering, Guilin University of Technology, Guilin, China. Her research interests include vehicle platoon control and disturbance observer-based control.

XUBIN TANG received the B.S. degree in automation from Guilin University of Technology, Guilin, China, in 2022. He is currently pursuing the master's degree with the College of Mechanical and Control Engineering, Guilin University of Technology, Guilin, China. His research interests include vehicle platoon control and multiagent systems.